Spark Ignition Feedback Control by Means of Combustion Phase Indicators on Steady and Transient Operation

Pipitone Emiliano
Dipartimento di Ingegneria Chimica, Gestionale, Informatica, Meccanica, University of Palermo, Palermo 90128, Italy
e-mail: emiliano.pipitone@unipa.it

In order to reduce fuel cost and CO_2 emissions, modern spark ignition (SI) engines need to lower as much as possible fuel consumption. A crucial factor for efficiency improvement is represented by the combustion phase, which in an SI engine is controlled acting on the spark advance. This fundamental engine parameter is currently controlled in an open-loop by means of maps stored in the electronic control unit (ECU) memory: such kind of control, however, does not allow running the engine always at its best performance, since optimal combustion phase depends on many variables, like ambient conditions, fuel quality, engine aging, and wear, etc. A better choice would be represented by a closed-loop spark timing control, which may be pursued by means of combustion phase indicators, i.e., parameters mostly derived from in-cylinder pressure analysis that assume fixed reference values when the combustion phase is optimal. As documented in literature, the use of combustion phase indicators allows the determination of the best spark advance, apart from any variable or boundary condition. The implementation of a feedback spark timing control, based on the use of these combustion phase indicators, would ensure the minimum fuel consumption in every possible condition. Despite the presence of many literature references on the use combustion phase indicators, there is no evidence of any experimental comparison on the performance obtainable, in terms of both control accuracy and transient response, by the use of such indicators in a spark timing feedback control. The author, hence, carried out a proper experimental campaign comparing the performances of a proportional-integral spark timing control based on the use of five different in-cylinder pressure derived indicators. The experiments were carried out on a bench test, equipped with a series production four cylinder spark ignition engine and an eddy current dynamometer, using two data acquisition (DAQ) systems for data acquisition and spark timing control. Pressure sampling was performed by means of a flush mounted piezoelectric pressure transducer with the resolution of one crank angle degree. The feedback control was compared to the conventional map based control in terms of response time, control stability, and control accuracy in three different kinds of tests: steady-state, step response, and transient operation. All the combustion phase indicators proved to be suitable for proportional-integral feedback spark advance control, allowing fast and reliable control even in transient operations. [DOI: 10.1115/1.4026966]

Keywords: spark advance, feedback control, combustion phase indicators, cylinder pressure, spark ignition engine

Introduction

Today's increasing fuel costs and demand for low CO_2 emission vehicles drive the development of higher efficiency engines.

Contributed by the Dynamic Systems Division of ASME for publication in the Journal of Dynamic Systems, Measurement, and Control. Manuscript received May 9, 2013; final manuscript received February 23, 2014; published online July 9, 2014. Assoc. Editor: Gregory Shaver.

As known, one of the most important parameters affecting internal combustion engine efficiency is represented by the combustion phase, which in a spark ignition engine is controlled by phasing the spark employed to start the combustion. In order to correctly phase the combustion with respect to the piston movement, the spark must be normally generated with a certain advance with respect to the top dead centre (TDC) position: the engine ECU, hence, usually performs an open-loop control of the combustion phase on the base of proper spark advance maps predetermined on bench tests and stored in memory. This system, however, presents some drawbacks, for instance:

- The spark advance mapping process is time consuming and subject to error.
- The mapping process can involve a finite number of operative conditions and, hence, cannot explore every load and speed condition.
- There may be differences between the test engine used for the mapping process and each single produced engine.
- Apart from the engine operative conditions, the best spark advance depends on many variables, such as the ambient pressure and temperature, air humidity, engine aging and wear, fuel quality, etc. [1].

A closed-loop control can overcome all of these problems, allowing to set the best spark advance regardless of any variable or boundary condition. The best (or optimal) spark advance is usually referred to as the maximum brake torque (MBT) spark advance since it allows maximizing engine torque, being constant for all the other conditions (i.e., engine speed, manifold pressure, air to fuel ratio, etc.); this also implies the maximum engine efficiency. If included in an automated test procedure, a feedback spark timing control would allow speeding up the mapping process, which is usually expensive and time consuming. The on-board implementation of such a control would allow a real-time optimization of the combustion phase for every engine speed and load, regardless of ambient condition, fuel quality, engine wear, etc.

A good process variable for the realization of such a control is represented by a combustion phase indicator, i.e., a parameter, usually derived from in-cylinder pressure analysis, whose value depends only on the combustion phase and assumes a fixed reference value when the combustion phase is optimal; the use of combustion phase indicators is well documented in literature and, as shown further on, allows performing fast and robust feedback control on engine spark timing. However, dealing with the closed-loop control of combustion phase, two main issues must be discussed: the first relates to the in-cylinder pressure sampling, which, requiring the use of a pressure sensor, may involve substantial additional costs if high precision transducers are considered. As mentioned further on, however, some of the combustion phase indicators taken into consideration by the author do not require high accuracy pressure measurement and may, hence, allow the feedback combustion control by the use of low cost in-cylinder pressure transducers, which are nowadays available for series production vehicles, as for example Refs. [2] and [3]. Furthermore, the evaluation of combustion phase indicators may be also pursued without pressure sampling, for example, by means of ionization current measurement, as described in Refs. [4] and [5].

The second issue is instead related to the dangerous knocking phenomena, which may occur in high load condition and compel retarding the combustion phase with respect to the optimal value: hence, depending on the fuel used (liquefied petroleum gas and compressed natural gas have higher knock resistance than standard gasoline) and on the engine characteristics (i.e., volumetric compression ratio) the feedback spark timing control system should be integrated by a proper knock onset diagnosis algorithm; it goes without saying that the same pressure sensor used to evaluate the combustion phase indicator could also be employed for knock diagnosis.

Although studies on the combustion phase indicators are diffused in literature, there is no trace of a comparison of the performance obtainable by such indicators when employed on a spark timing feedback control. The author, hence, taking into account five different combustion phase indicators derived from in-cylinder pressure analysis, carried out proper experimental tests comparing their behavior in terms of both control accuracy and transient response when employed in a feedback spark timing control.

Combustion Phase Indicators

In the past, different techniques were proposed for the optimal tuning of spark advance, mainly based on the in-cylinder pressure analysis. These methods substantially rely on the use of *combustion phase indicators*, namely parameters, usually derived from the in-cylinder pressure, which assume fixed reference values when spark timing is set to the MBT value. In the present paper, five different combustion phase indicators have been taken into account for the comparative tests:

(1) location of pressure peak (LPP)
(2) location of maximum pressure rise (LMPR)
(3) location of 50% of mass fraction burned (MFB50)
(4) location of maximum heat release rate (LMHR)
(5) value of relative pressure ratio 10 crank angle degree after top dead centre (ATDC) (PRM10)

The first four indicators are evaluated in terms of crank angle degrees (CAD) ATDC, while the fifth is a dimensionless number.

The location of the pressure peak concept is well known and has been widely used in adaptive spark timing control studies [1,6–11]: according to this method, under MBT spark timing, the combustion chamber pressure reaches its maximum at approximately 14-16 crank angle degrees after TDC.

Also, the method of the location of maximum pressure rise was documented a long time ago [12]: the best spark advance is obtained when the crank angle of the maximum pressure rise rate is around 3 crank angle degrees ATDC, independent of mixture strength and other boundary conditions.

Another known combustion descriptor is the crank angle at which the 50% of fuel mass is burned (MFB50): this should happens around 9 crank angle degrees ATDC when running with the optimal spark timing [1,13–15]. With respect to the first two parameters, the MFB evaluation requires heavier computation [16–21] besides a precise pressure measurement; if the transducer used does not assure an absolute indication (as for example happens employing an uncooled piezoelectric sensor), a pressure referencing technique must be adopted; some useful indications can be found in Refs. [22] and [23].

The location of maximum heat release rate, reported in Refs. [24] and [25], is not frequently cited in literature as combustion phase indicator. If the classical Wiebe function for combustion heat release is considered, the LMHR should nearly correspond to the MFB50; it could be considered a valid alternative to MFB50 since it is much less sensitive to transducer bias error or pressure referencing uncertainty and does not require any extra computational effort.

Very similar to the MFB concept is the pressure ratio management (PRM), introduced by Matekunas et al. [26]: it is based on the same principle of the MFB calculated by Rassweiler and Withrow [16], i.e., the fractional pressure rise due to combustion; Matekunas defined the pressure ratio as the ratio between the measured and the "motored pressure" (which would exist without combustion), the latter obtained by a polytropic law. It consists practically in a simpler version of the mass fraction burned algorithm and often gives the same values: it also shares the same weak point, i.e., the necessity for precise pressure measurement or referencing. The indicator that Matekunas suggests to take into

Table 1 Preliminary tests results (1500–3500 rpm, 3 and 6 bar BMEP, $\lambda = 1$)

Indicator	Mean optimal value	Range of dispersion
LPP	15	3.2
LMPR	4	4.0
MFB50	8	4.2
LMHR	8	4.6
PRM10	0.58	0.20

consideration is the PRM10, defined as the value that PRM assumes 10 crank angle degrees ATDC

$$\text{PRM10} = \frac{\text{PR}(10) - 1}{\text{PR}(55) - 1}$$

where PR(55) is the pressure ratio value at 55 crank angle degrees ATDC, i.e., approximately the final pressure ratio.

The PRM10 is the only combustion phasing indicator considered here to be expressed in nondimensional value: it ranges from 0 to 1 and, as suggested by its author [26], when running with the best spark advance it should be equal to 0.55.

The reference (or optimal) value of each indicator is an experimental fact and should be determined by proper experimental tests as the mean of the values measured over a wide number of engine operative condition. Lacking this information, however, the values mentioned above can be considered valid references for every spark ignition engine.

Preliminary Test and Experimental Setup

All the combustion phase indicators presented can be calculated once the in-cylinder pressure as a function of the crank angle is known. Before implementing them on a real-time spark advance feedback control, it was decided to experimentally estimate their optimal values, and, thus, some preliminary tests were carried out, acquiring the cylinder pressure with varying spark advance, for different conditions of load (3 and 6 bar brake mean effective pressure (BMEP)) and speed (from 1500 to 3500 by step of 200 rpm): higher loads were not explored since knocking phenomena limit the spark timing optimization. The test bench was equipped with a series production Renault 1598 cc four cylinders spark ignition engine connected to a Schenck eddy current dynamometer. The engine was endowed with an AVL GU13Z-24 piezoelectric pressure transducer, flush mounted in the combustion chamber by means of its spark plug adaptor ZF42, and a 360 pulses per revolution incremental optical encoder was used to clock the analog acquisition with a resolution of 1 crank angle degree. The data were collected through a National Instrument 6062 DAQ card properly programmed in LABVIEW environment. During these preliminary tests the spark timing was varied around the MBT condition by means of a computer controlled ECU, while the air-to-fuel ratio was kept to the stoichiometric value.

As mentioned before, absolute pressure values are necessary when performing heat release analysis. Hence, for a correct evaluation of MFB50, PRM10, and LMHR, the output of the uncooled pressure transducer employed was referenced. The two most suitable referencing techniques were considered [22,23]: the inlet manifold pressure based and polytropic index based. The first method assumes that in-cylinder pressure around the intake BDC is equal to the manifold absolute pressure (MAP); this requires the use of a MAP sensor, which is commonly integrated in modern spark ignition engine management systems. The second method instead forces the compression polytropic index to a fixed value, which should lie between 1.28 and 1.32. In the tests performed, in-cylinder pressure was referenced by means of the manifold absolute pressure measured by a DRUCK PMP 1400 piezoresistive sensor. A fundamental prerequisite for a correct

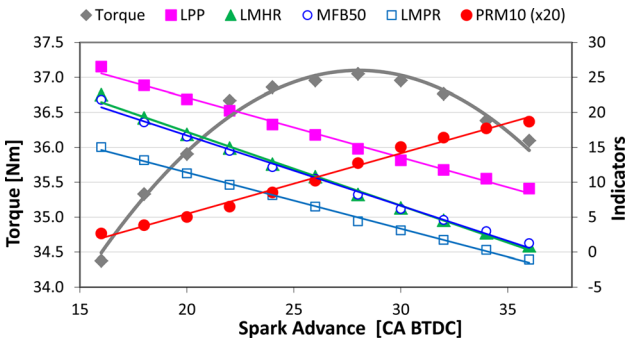

Fig. 1 Combustion phase indicators and engine torque as function of spark advance (1900 rpm, 3 bar BMEP, $\lambda = 1$)

evaluation of combustion phase indicators is represented by the determination of the TDC position, which should be carried out within the accuracy of 0.1 CAD. As an alternative to dedicated sensors, such as the Kistler 2629B used by the author, different thermodynamic methods can be employed [27,28] for the purpose.

In order to remove unwanted mechanical and electrical noise from the in-cylinder pressure signal a fourth-order Butterworth filter with zero phase shift (which is a fundamental prerequisite dealing with combustion phasing analysis) was used, while engine cycle-by-cycle variations, which strongly affect the measurement of the combustion phase indicators, were overcome by computing each indicator on the base of the mean pressure cycle evaluated over 50 consecutive cycles.

The results of the first series of tests are collected in Table 1: here, the mean optimal value is shown for each indicator together with its range of dispersion. It can be noted that, among the indicators measured in crank angle degrees, the LPP exhibits the lowest dispersion and that LMHR and MFB50 show the same optimal values with almost equal dispersions.

It was also found to exist a good linear correlation between indicators and spark advance, as shown in Fig. 1: this is a desirable feature for spark timing feedback control. The same figure also shows how LMHR and MFB50 share a higher slope compared to LPP and LMPR: this denotes a higher sensitivity to spark advance, which could permit a more precise control over spark timing.

The data collected during these preliminary tests permitted evaluation of the deviation induced on MFB50, LMHR, and PRM10 (LPP and LMPR are intrinsically not influenced) by the pressure referencing error, which is one of the most common uncertainty related to in-cylinder pressure measurement. As can be seen in Fig. 2, the referencing error strongly affects both MFB50 and PRM10, while wields a light influence on LMHR. This makes LMHR preferable to MFB50.

Feedback Spark Advance Control

Once their optimal values were determined, the indicators were implemented as process variables on a feedback control system, which was realized [29] by the use of a second DAQ board, whose role was to receive the spark timing information from the first DAQ board (which performed all the data acquisition and processing) and send the consequent digital pulses to two automotive ignition power transistors (one for every couple of cylinders). The transistors converted the low energy TTL signals into a high energy waveforms, thus causing the sparks to occur at the desired instants (see Fig. 3).

A proportional integral derivative (PID) controller was chosen among the feedback control structures for its simplicity and robustness. In the general structure of a feedback control, as represented in Fig. 4, the controller compares the actual value of the controlled variable (the engine pressure derived indicator) with its set point (the MBT value) and obtains an error, on the base of

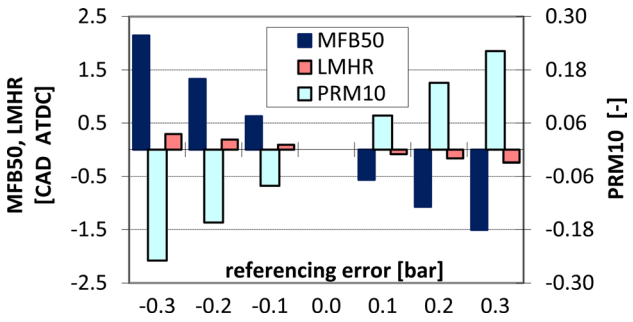

Fig. 2 Indicator evaluation error due to pressure referencing error (2500 rpm, 3 bar BMEP, $\lambda = 1$)

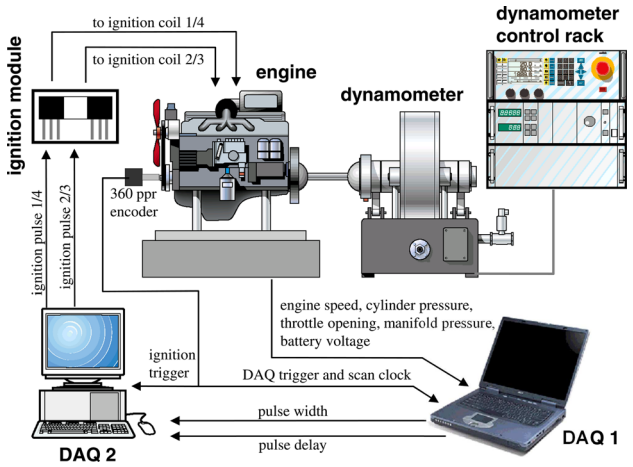

Fig. 3 Experimental setup

which performs an adjustment on the output (spark advance) that in turn causes a change on the engine pressure and, hence, on the indicator value.

The output of a general PID controller is directly proportional to the error by the constant K_P, to the integral of the error by the constant K_I and to the derivative of the error by the constant K_D, hence

$$\mathrm{SA} = K_P \cdot e(t) + K_I \cdot \int e(t) \cdot dt + K_D \cdot \frac{\partial e(t)}{\partial t}$$

where $e(t)$ is the error (function of time t).

As is known, a simple proportional control would not be successful since a steady-state error (also named offset error) would persist. The integral action is effective in forcing the steady-state error to zero because it is proportional to the accumulated error. The derivative action should have a predictive effect, being proportional to the rate of change of the controlled variable; the drawback in the use of the derivative control action is the tendency to yield large output oscillations in response to high frequency errors induced by measurement noise, which is quite the case of the variables here controlled (the pressure derived indicators): due to engine cycle-by-cycle variation, in effect, each combustion phase indicator is characterized by strong noise effect (as can be seen in Fig. 5).

In order to prevent the control system from producing excessive spark advance oscillations, it was decided to work on the base of a moving average pressure cycle calculated over 20 consecutive engine cycles: this was considered a good compromise between the use of a 50 cycles average (as in the preliminary tests), which yields a marginal oscillations but introduces high response delay

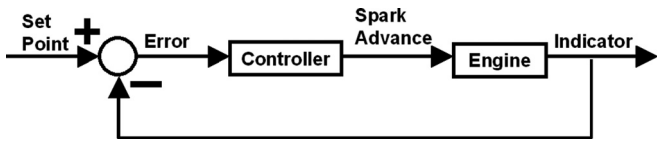

Fig. 4 Feedback control structure

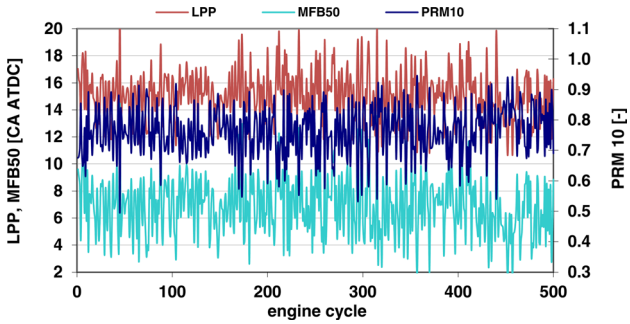

Fig. 5 LPP, MFB50, and PRM10 evaluated on single pressure cycle with constant spark advance operation (2500 rpm, 50 Nm, $\lambda = 1$)

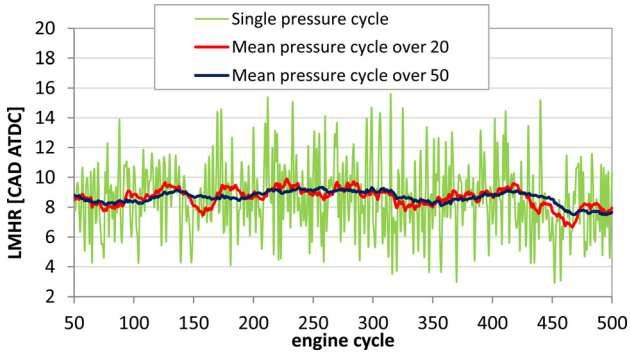

Fig. 6 Progress of LMHR measured both on single pressure trace and mean pressure trace evaluated over 20 and 50 consecutive pressure cycles

to changing conditions, and the evaluation on the base of each single pressure cycle, which, against a null response delay, causes too wide and high frequency oscillations, as remarked by Fig. 6.

From now onwards the value of each indicator has been determined on the base of a mean pressure trace evaluated over 20 consecutive engine cycles.

The controller parameters K_P, K_I, and K_D have a great influence on the control performance and can be tuned, at least as initial stage, by means of practical rules, for example, the reaction curve based method or the oscillation method [30]. In this work, the coefficients for the controller were tuned by means of the first technique, which relies on the analysis of the reaction of the system when subjected to a step perturbation under open-loop control: Fig. 7 shows the response of the MFB50 indicator to a 10 deg step variation of the spark advance.

The technique gave good results as regards the coefficients K_P and K_I, while the derivative action, as warned above, caused undesirable and dangerous high frequency spark advance oscillations, as can be seen in the upper graph in Fig. 8: here the progress of LPP and spark advance are shown for a steady-state operation under PID control; the measured overall spark advance fluctuation was as high as 12 deg, while LPP remained in the range ± 1 from the set point (broken lines delimit the reference benchmark reported in Table 3). In order to overcome these excessive spark

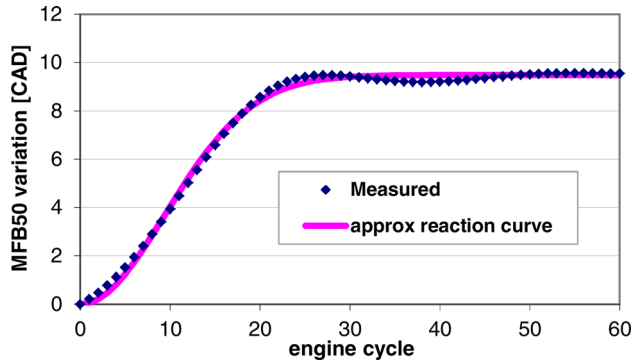

Fig. 7 Reaction curve for a step spark advance increment of 10 deg (which starts at cycle 0) of the MFB50 (evaluated on the base of 20 cycles mean pressure trace)

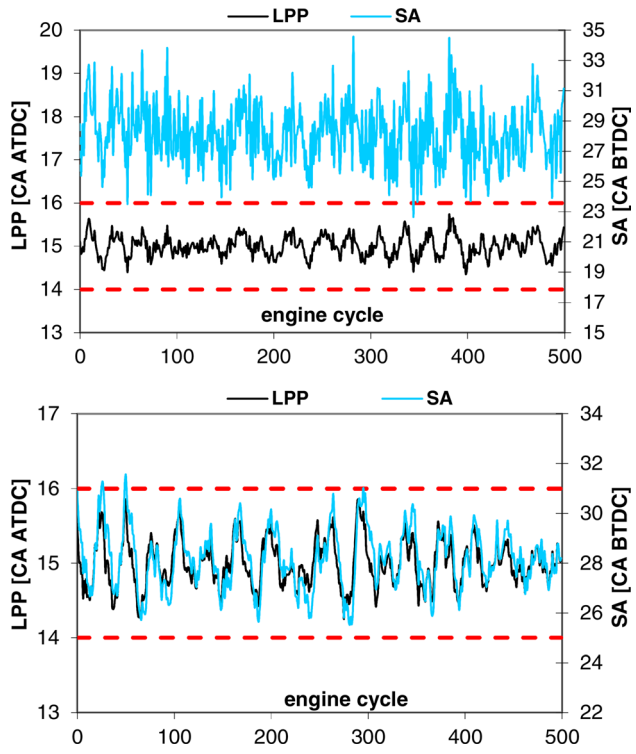

Fig. 8 Fluctuation of both spark advance and LPP (evaluated on 20 cycles mean pressure trace) in steady-state operation with PID (top) and PI (bottom) control

advance fluctuations it was decided to eliminate the derivative action, thus using a proportional integral control. This lowered the spark advance oscillation both in amplitude, which dropped to 6 degrees, and in frequency, as can be observed in the lower graph in Fig. 8.

The coefficients obtained for the PI controller by means of the Cohen and Coon reaction based method [30] are summarized in Table 2. As can be noted, all the indicators expressed in terms of crank angles (LPP, LMPR, MFB50, and LMHR) are characterized by similar values, even if the largest difference has been unexpectedly found for the two most similar indicators, i.e., MFB50 and LMHR; PRM10, instead, being, as already mentioned, a dimensionless parameter ranging between 0 and 1, gave, as expected, quite different tuning coefficients; all the indicators, however, show the existence of an optimal ratio between the K_P and K_I, which is roughly 10.

The lower graph in Fig. 8 shows how the PI controller pursued the indicator variations, which caused the 6 deg spark advance

Table 2 Tuned PI controller coefficients (Cohen and Coon reaction based method)

Indicator	K_P	K_I
LMPR	3.25	0.30
LPP	3.12	0.33
MFB50	3.82	0.44
LMHR	2.38	0.22
PRM10	78.5	9.8

Table 3 Spark advance and indicator fluctuations measured in the steady-state tests

	PI feedback control				
Fluctuation	LPP	LMPR	MFB50	LMHR	PRM10
SA	3.5	3.7	3.9	4.3	3.2
Indicator	1.4	1.7	2.0	1.7	0.08
	Fixed SA control				
Fluctuation	LPP	LMPR	MFB50	LMHR	PRM10
SA	0	0	0	0	0
Indicator	2	2.6	2.6	2.6	0.12

oscillations. A further improvement was made by implementing a simple spark advance filter that limits its changes when the error is small. This allowed the overall spark advance fluctuation to remain in the acceptable range of 3-4 deg and was used in all the tests. Once established the controller parameters, each indicator was tested in three different ways: steady-state control, step response, and transient control.

Steady-State Tests

This first series of tests aimed to prove the controller stability and accuracy. The system was put in closed-loop control at 2500 rpm and 6 bar BMEP and its capability to keep the indicators value (evaluated on a 20 cycles mean pressure trace) next to its optimal value was verified; the terms of comparisons were the overall fluctuation (i.e., the peak to peak value) of both spark advance and indicator value, whose progress was recorded over 500 cycles. The benchmarks were fixed by the indicator fluctuations measured during open-loop operation with fixed spark advance, at the same load and speed conditions (last row in Table 3). As an example, Fig. 9 shows the result of the PRM10 steady-state test. Here, the progress of both spark advance and indicator value are reported for 500 consecutive engine cycles. As can be seen, not only the feedback PI control successfully maintained the indicator between the two benchmark broken lines but also performing continuous adjustments on the spark timing in order to maintain the PRM10 as near as possible to the set point value. Also, it obtained a lower indicator fluctuation with respect to the constant spark advance operation. This result was repeated by each of the indicators, as shown in Table 3 and Fig. 10. In conclusion, in steady-state operation, the PI feedback control ensures the best performance together with lower indicator fluctuation with respect to fixed spark advance control. The spark advance fluctuation ranged from 3 deg for the PRM10 to 4 deg both for MFB50 and LMHR. As regards the last two indicators, this first series of tests showed almost equal performances.

Step Response Tests

These tests aimed to evaluate the speed of response of the feedback control system in finding the best spark timing when forced to start from a steady-state error configuration. This may occur for

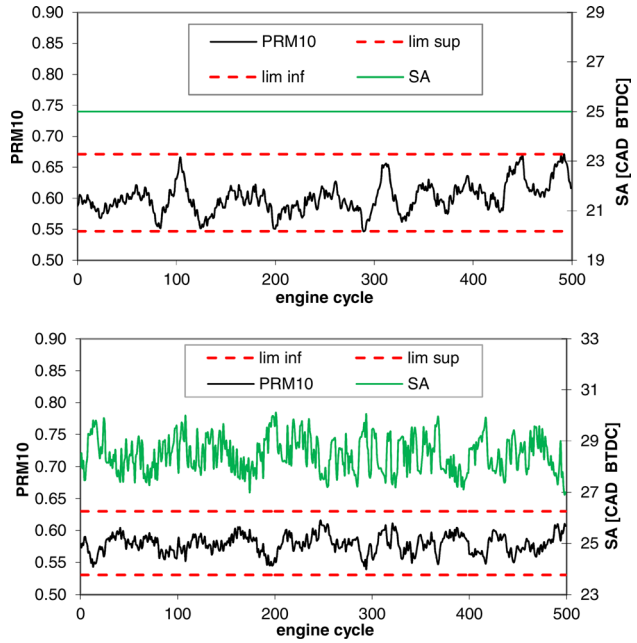

Fig. 9 PRM10 steady-state test results for fixed SA operation (upper graph) and closed-loop SA control (lower graph); broken lines delimit the benchmark window

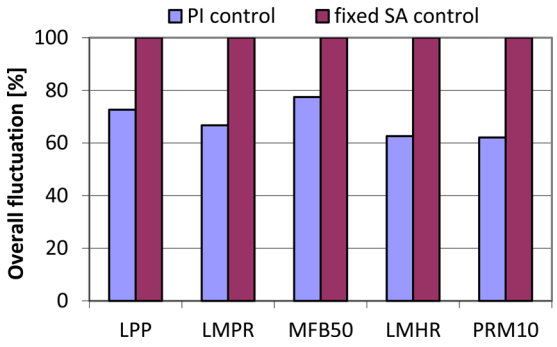

Fig. 10 Indicator fluctuations comparison between PI and fixed spark advance control in steady-state tests

a sudden load and/or speed variation, or during a mapping process.

The engine operative conditions were 2500 rpm and 6 bar BMEP, and the step perturbation was realized running the engine in open-loop control with an initial spark advance 5 deg lower than MBT and then switching to the closed-loop control. The indicator evaluation was performed on the base of the 20 cycles averaged pressure cycle. The response of the control system was recorded (see, for example, Fig. 11) and analyzed for the evaluation of the two most significant parameters: the *cycles to window* C_W, that is the number of engine cycles the controller takes to definitively bring the indicator value inside the benchmark window (assumed equal to the steady-state tests), and the *cycles to zero* C_Z, which instead represents the number of engine cycles needed for the first zero of the error (which is the difference between the indicator set point and the actual indicator value, as shown in Fig. 4). The overall results of these tests are summarized in Table 4. All the combustion phase descriptors gave fast responses with the PI control. The LMPR demonstrated to be the "slowest," taking 17 cycles to reach the target; the differences between indicator rising times are negligible. Above all if it is considered that for each indicator, the controller parameter K_P and K_I were set by means of an empirical rule and were not optimized. A more accurate tuning would probably give better and more uniform

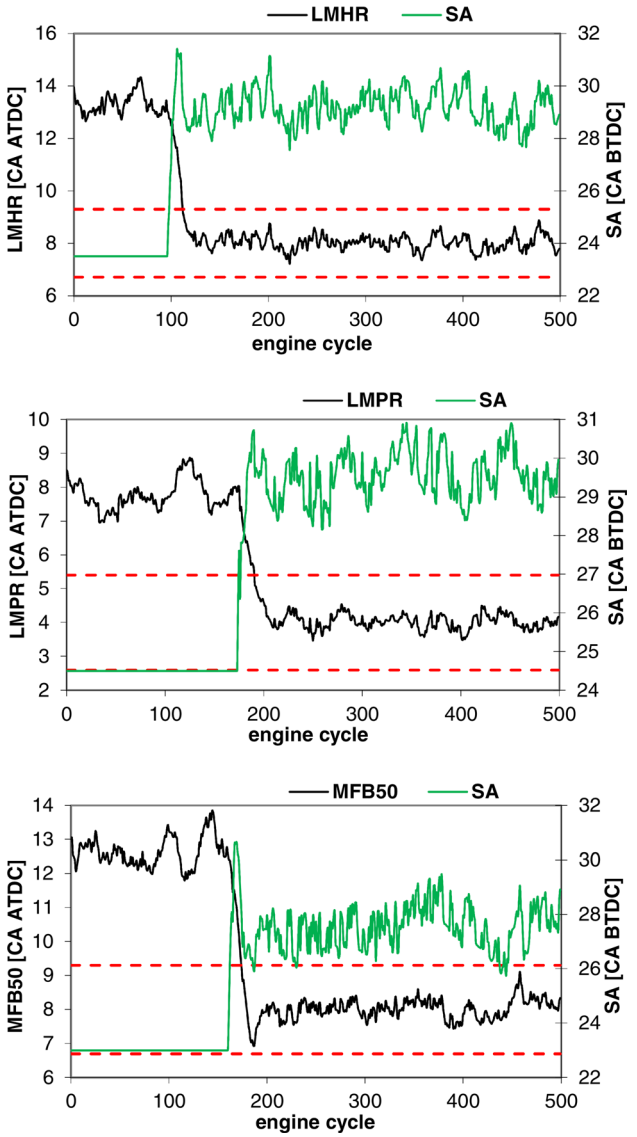

Fig. 11 LMHR, LMPR, and MFB50 step response results (broken lines indicate the benchmark window)

Table 4 Overall results of the step response tests

	PI control				
Indicator	LPP	LMPR	MFB50	LMHR	PRM10
Set point	15	4	8	8	0.58
Benchmark	±1.4	±1.4	±1.7	±1.8	±0.06
C_W	13	17	12	14	12
C_Z	23	34	19	29	19

results. The same conclusions can be approximately drawn for the *cycles to zero*. The notable result is that, as can be seen in Table 4, for a 5 deg spark advance step, the *cycles to window* are always lower than 20, which is the number of engine cycles needed to completely update the indicator value after the step change. This means that the controller response is fast enough, apart from the used indicator.

Transient Tests

A pure feedback control, which namely does not make use of any stored map, can undergo instability or cause wide fluctuations

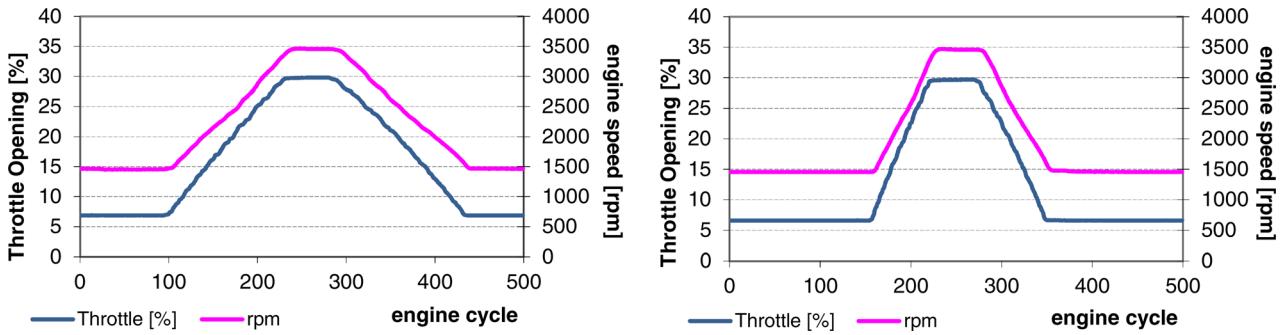

Fig. 12 Engine speed and throttle opening in slower (on the left) and faster (on the right) transient operations

of the indicators during transient operation, as a result of the changing conditions of engine load and/or speed. It was then decided to simulate on road accelerations and decelerations in order to evaluate the stability of the feedback control during transient operations. For the purpose, the eddy current dynamometer was set to a "road load" type braking characteristic and two different throttle opening laws were realized by means of a motor driven throttle actuator installed on the engine test bed: in the slower transient, the engine speed raised from 1500 to 3500 rpm (and the torque from 20 to 80 Nm) within 7 s, while half the time was required by the faster transient. In Fig. 12, the throttle opening laws and the resulting engine speed are shown for both the transients performed.

The aim of these tests was to ascertain the capability of the simple feedback control realized to maintain a stable control on spark advance even during transient operation, without causing too wide indicators fluctuation; as reference to establish a tolerable amplitude of the indicators fluctuations, it has been decided to refer to the good map based control performed by the original ECU of the engine used for the test, which has been programmed and calibrated by expert staff in order to correctly follow load and speed transients. In the tests carried out, hence, the amplitude of the

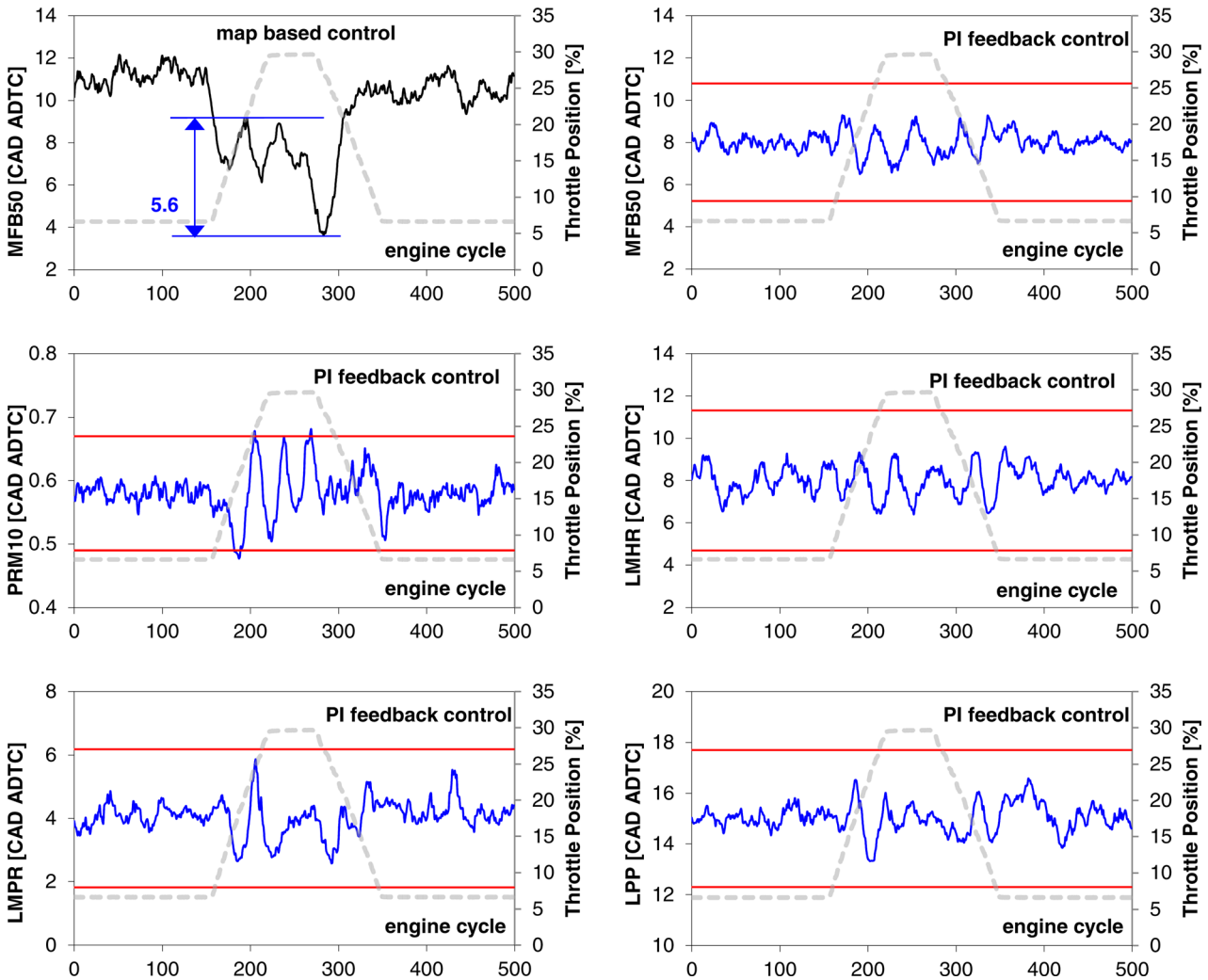

Fig. 13 Result of the faster transient test (horizontal lines delimit benchmark window, dashed line represents throttle position)

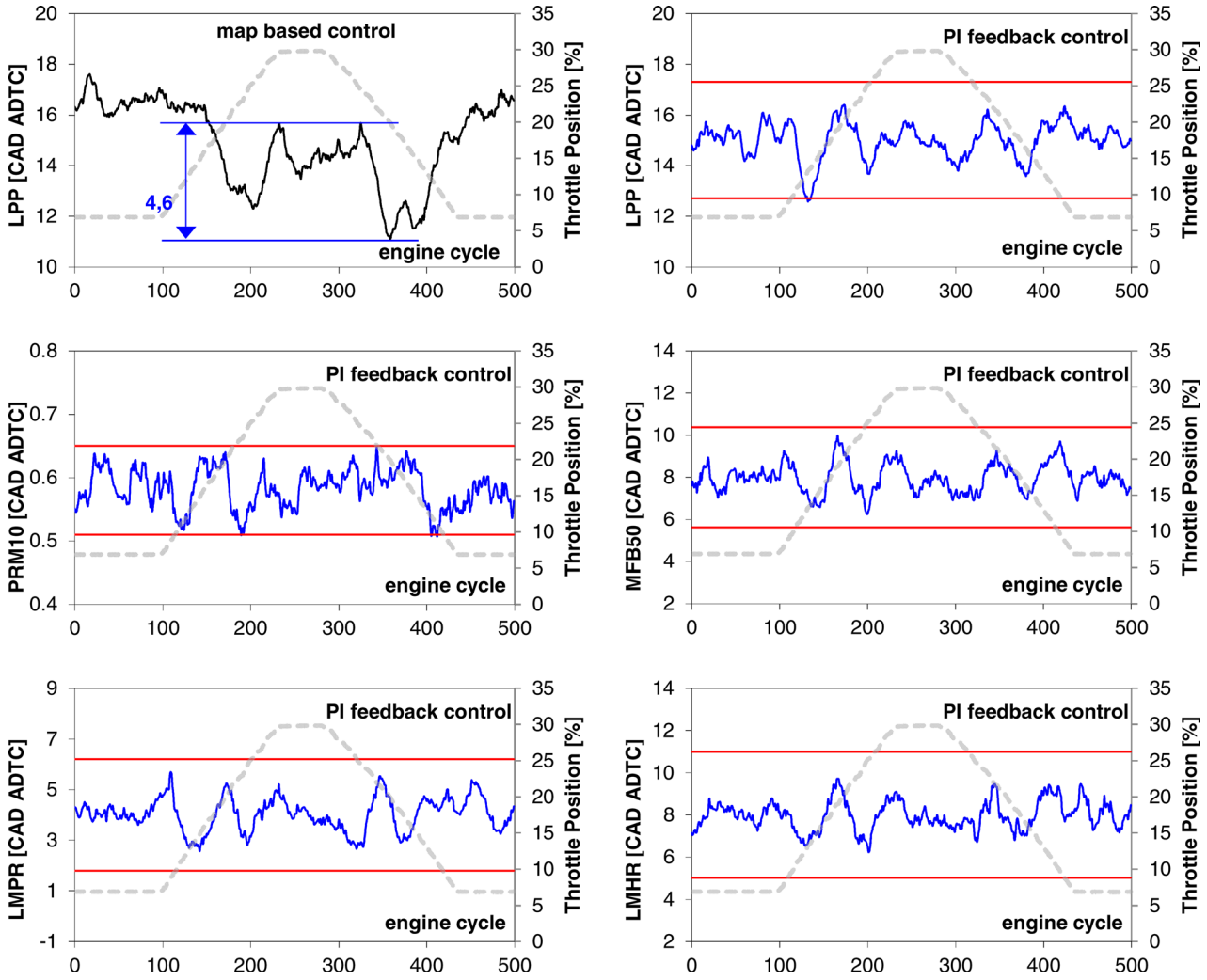

Fig. 14 Result of the slower transient test (horizontal lines delimit benchmark window, dashed line represents throttle sition)

indicators fluctuations measured using the original ECU have been chosen to trace the benchmark windows. The transient tests has been considered successfully passed when the feedback controller succeeded in maintaining each indicator inside the reference benchmark window. The faster and the slower transient tests, hence, were performed both in the feedback control mode and in the map based control mode and the progress of each indicator (evaluated on the base of a 20 cycles averaged pressure trace) has been recorded. The result of these tests is shown in the diagrams of Figs. 13 and 14, respectively; on each diagram, the progress of the measured indicator is reported together with the throttle opening law, represented by a dashed line, and the two horizontal lines delimiting the benchmark window.

The first diagram in Fig. 13 reports the MFB50 measured during the spark timing control of the series production ECU, while the other diagrams reports the progress of each indicator during the PI feedback spark timing control. As regards the MFB50 in map based control, it can be observed that an initial steady-state error (about 3 CAD) is present both before the throttle starts to open and after the throttle has terminated its closing phase; this means that the map based control performed by the original series production ECU is not optimal at the minimum load since the indicator is not at its best value. This, however, has no significance in these kind of tests since the only relevant output from original ECU control is represented by the amplitude of the indicator fluctuation during transient operation, which has been assumed as validating reference for the evaluation of the PI feedback control stability.

Moreover, as can be seen in Fig. 13, the presence of the initial and final steady-state errors may lead to a misleading calculation of the indicator range of variation. For this reason, for the map based control, the amplitude of each indicator fluctuation has been evaluated considering only the inner part of the diagram, completely excluding the steady-state errors effects.

As regards the proportional integral feedback control, the results of the transient tests show a very good stability of the control system, which not only did not cause any instability phenomena but also succeeded in maintaining all the indicators inside the benchmark window (delimited by the two horizontal lines), as confirmed by the results summarized in Tables 5 and 6. Here, the range of variation of each indicator measured in the two transient tests is reported.

Table 5 Indicators range of variation during slower transient operation

	LPP	LMPR	MFB50	LMHR	PRM10
PI control	3.83	3.13	3.74	3.50	0.14
Map based control	4.59	4.40	4.76	5.99	0.14

Table 6 Indicators range of variation during faster transient operation

	LPP	LMPR	MFB50	LMHR	PRM10
PI control	3.26	3.28	2.79	3.21	0.20
Map based control	5.41	4.37	5.56	6.63	0.18

As can be observed, the PRM10 gave rise to fluctuation as high as those measured in map based mode, while all the other indicators allowed performance of better control of the spark timing during the transient operation with respect to the original ECU.

It is worth mentioning that the range of variation measured for each of the five different indicators during the feedback control on transient operations resulted in similar or even lower than the range of dispersion of the indicators values determined in the preliminary tests and shown in Table 1, which represent the statistical dispersions of the data used to compute each optimal indicator value.

In conclusion, the simple proportional integral spark timing control realized, once tuned by means of a practical rule, allowed performing a sufficiently stable control on spark advance even in transient operations, maintaining each indicator inside an acceptable range of variation.

Conclusions

Feedback controls may be implemented in spark ignition engines for combustion phase control, in order to maximize engine efficiency for any operative or boundary conditions, or simply speed up the mapping processes carried out in the engine test beds. The aim of this work was hence to realize a simple feedback spark timing control to test and compare to conventional open-loop map based control. A proportional integral (PI) spark timing control system using in-cylinder pressure based combustion phase indicators as process variables has been realized and its performance in terms of control accuracy, speed of response, and control stability have been tested in three different kinds of test: steady-state, step response, and transient operation.

The main obstacle in the pressure based feedback spark timing control of the engine was found in the measurement disturbance related to cycle-by-cycle variations: this discouraged the use of a derivative control action and forced to evaluate each indicator on the base of a moving averaged pressure trace evaluated over 20 consecutive engine cycles: the drawback of this filtering method is that it may slow down the system response.

Five different combustion phase descriptors (LPP, LMPR, MFB50, LMHR, and PRM10) were considered, in order to perform a comparison, and a good linear relation was found between each of them and the spark advance: this constitutes a desirable feature for feedback control. For each of the indicators, the coefficients of the PI controller were tuned by means of the Cohen & Coon reaction based method.

All the combustion phase indicators proved to be suitable for PI feedback spark advance control, showing good control accuracy in the steady-state tests and a sufficiently high speed of response in the step response tests, above all if the slowing effect produced by the moving average filter employed is considered. On-road accelerations and decelerations have also been simulated on the engine test bed in order to test the stability of the feedback control in transient operations. As a reference, the stability performance of the map based control performed by the original ECU of the engine was chosen: according to the results obtained, each of the tested indicators proved to maintain a stable control on spark advance also during transient operations.

The choice between indicators can be influenced by economic factors and/or the ease of use: LPP and LMPR do not require absolute pressure values, and so are suitable for the use with low cost pressure sensors, nowadays available for the series production engine market [2,3]; moreover, due to the small amount of data needed for their evaluation (in-cylinder pressure must be sampled for an interval of 60 CAD around the TDC), the evaluation of both LPP and LMPR also require the lowest amount of calculus.

On the contrary, the indicators related to heat release analysis, i.e., MFB50, LMHR, and PRM10, not only require the sampling of the whole in-cylinder compression and expansion phases but also involve heavier calculations. Moreover, the evaluation of both MFB50 and PRM10 needs accurate in-cylinder pressure measurement. The opportunity of substituting the MFB50 with the LMHR, less cited in literature, was also considered. These two parameters, according to the S-shaped function of the heat released by combustion, give the same information and share almost equal results. The advantages of LMHR with respect to MFB50 rely on its much lower sensitivity to pressure referencing error, which makes it suitable for the use with low cost pressure sensors.

Acknowledgment

The author gratefully thanks Renault Italia for the engine supply and Mr. Beniamino Drago for the indispensable technical support and the realization of the engine test bench.

Nomenclature

λ = relative air-fuel ratio = (actual A/F)/(stoichiometric A/F)

Abbreviation

A/F = air-fuel ratio
ATDC = after top dead centre
BDC = bottom dead centre
BMEP = brake mean effective pressure
BTDC = before bottom dead centre
CA = crank angle
CAD = crank angle degree
CNG = compressed natural gas
DAQ = data acquisition
ECU = electronic control unit
LMHR = location of maximum heat release rate
LMPR = location of maximum pressure rise
LPG = liquefied petroleum gas
LPP = location of pressure peak
MAP = manifold absolute pressure
MBT = maximum brake torque
MFB = mass fraction burnt
MFB50 = location of 50% of mass fraction burnt
PI = proportional integral
PID = proportional integral derivative
PR = pressure ration
PRM10 = pressure ration management value 10 crank angle degrees ATDC
SA = spark advance
TDC = top dead centre

References

[1] Pestana, G. W., 1989, "Engine Control Methods Using Combustion Pressure Feedback," SAE Paper No. 890758.
[2] BERU Pressure Sensor Glow Plug (PSG) for Diesel Engines, http://beru.federalmogul.com
[3] Sensata CPOS SERIES—Cylinder Pressure Only Sensors, http://www.sensata.com/download/cpos.pdf
[4] Malaczynski, G., Roth, G., and Johnson, D., 2013, "Ion-Sense-Based Real-Time Combustion Sensing for Closed-Loop Engine Control," SAE Int. J. Eng., **6**(1), pp. 267–277.
[5] Henein, N. A., Bryzik, W., Abdel-Rehim, A., and Gupta A., 2010, "Characteristics of Ion Current Signals in Compression Ignition and Spark Ignition Engines," SAE Int. J. Eng., **3**(1), pp. 260–281.
[6] Yoshihisa, K., Mamoru, S., Hiroshi, S., Nobutaka, T., and Masahiro, I., 1988, "MBT Control Through Individual Cylinder Pressure Detection," SAE Paper 881779.

[7] David Powell, J., 1993, "Engine Control Using Cylinder Pressure: Past, Present, and Future," ASME J. Dyn. Syst., Meas. Control, **115**, pp. 343–350.
[8] Muller, R., Hart, M., Truscott, A., Noble, A., Krotz, G., Eickhoff, M., Cavalloni, C., and Gnielka, M., 2000, "Combustion Pressure Based Engine Management System," SAE Paper 2000-01-0928.
[9] Yoon, P., Park, S., Sunwoo, M., Ohm, I., and Yoon, K. J., 2000, "Closed-Loop Control of Spark Advance and Air-Fuel Ratio in SI Engines Using Cylinder Pressure," SAE Paper 2000-01-0933.
[10] Eriksson, L., 1999, "Spark Advance Modeling and Control," Dissertation N° 580, Linkoping Studies in Science and Technology, Linköping, Sweden.
[11] Samir, S., Agarwal, P. K., and Satish, C., 2011, "Neural Networks and Fuzzy Logic-Based Spark Advance Control of SI Engines," Expert Syst. Appl., **38**, pp. 6916–6925.
[12] Cook, H. A., Heinicke, O. H., and Haynie, W. H., 1947, "Spark-Timing Control Based on Correlation of Maximum-Economy Spark Timing, Flame-Front Travel, and Cylinder Pressure Rise," NACA Technical Note 1217.
[13] Bargende, M., 1995, "Most Optimal Location of 50% Mass Fraction Burned and Automatic Knock Detection," MTZ, **10**(56), pp. 632–638.
[14] Leonhardt, S., Muller, N., and Isermann, R., 1999, "Methods for Engine Supervision and Control Based on Cylinder Pressure Information," IEEE/ASME Trans. Mechatronics, **4**(3), pp. 235–245.
[15] Beccari, A., Beccari, S., and Pipitone, E., 2010, "An Analytical Approach for the Evaluation of the Optimal Combustion Phase in Spark Ignition Engines," ASME J. Eng. Gas Turbines Power, **132**(3), p. 032802, DOI: 10.1115/1.3155395.
[16] Rassweiler, G. M., and Withrow, L., 1938, "Motion Pictures of Engine Flames Correlated With Pressure Cards," SAE Paper 800131.
[17] Amann, C. A., 1985, "Cylinder Pressure Measurement and Its Use in Engine Research," SAE Paper 852067.
[18] Stone, C. R., and Green-Armytage, D. I., 1987, "Comparison of Methods for the Calculation of Mass Fraction Burnt From Engine Pressure-Time Diagrams," Proc. IMechE, **201**(1), pp. 61–67.
[19] Shayler, P. J., Wiseman, M. W., and Ma, T., 1990, "Improving the Determination of Mass Fraction Burnt," SAE Paper 900351.
[20] Brunt, M. F., Rai, H., and Emtage, A. L., 1998, "The Calculation of Heat Release From Engine Pressure Data," SAE Paper 981052.
[21] Ball, J. K., Raine, R. R., and Stone, C. R., 1998, "Combustion Analysis and Cycle-by-Cycle Variations in Spark Ignition Engine Combustion: Parts 1 and 2," Proc. IMechE, **212**, pp. 381–399.
[22] Randolph, A. L., 1990, "Methods of Processing Cylinder-Pressure Transducer Signals to Maximize Data Accuracy," SAE Paper 900170.
[23] Brunt, M. F. J., and Pond, C. R., 1997, "Evaluation of Techniques for Absolute Cylinder Pressure Correction," SAE Paper 970036.
[24] Pipitone, E., 2008, "A Comparison Between Combustion Phase Indicators for Optimal Spark Timing," ASME, J. Eng. Gas Turbines Power, **130**(5), p. 052808, DOI: 10.1115/1.2939012.
[25] Pipitone, E., and Beccari, A., 2007, "A Study on the Use of Combustion Phase Indicators for MBT Spark Timing on a Bi-Fuel Engine," SAE Technical Paper 2007-24-0051, DOI: 10.4271/2007-24-0051.
[26] Matekunas, F. A., Battiston, P. A., Chang, C. F., Sellnau, M. C., and Lancaster, D. R., 2000, "Cylinder-Pressure-Based Engine Control Using Pressure-Ratio-Management and Low-Cost Non-Intrusive Cylinder Pressure Sensor," SAE Paper 2000-01-0932.
[27] Pipitone, E., and Beccari, A., 2010, "Determination of TDC in Internal Combustion Engines by a Newly Developed Thermodynamic Approach," Appl. Therm. Eng., **30**(14), pp. 1914–1926, DOI: 10.1016/j.applthermaleng.2010.04.012.
[28] Pipitone, E., Beccari, A., and Beccari, S., 2008, "Reliable TDC Position Determination: A Comparison of Different Thermodynamic Methods Through Experimental Data and Simulations," SAE Paper 2008-36-0059, DOI: 10.4271/2008-36-0059.
[29] Pipitone, E., and Beccari, A., 2003, "A Real Time Platform for Feedback Spark Advance Control," Proceedings of the 58 ATI Congress, Italy.
[30] Goodwin, G. C., Graebe, S. F., and Salgado, M. E., 2000, *Control System Design*, Prentice Hall PTR, Upper Saddle River, NJ.